The Fidelity of NCEP CFS Seasonal Hindcasts over Nordeste

VASUBANDHU MISRA

Center for Ocean–Land–Atmosphere Studies, Institute of Global Environment and Society, Inc., Calverton, Maryland

YUNING ZHANG

Montgomery Blair High School, Silver Spring, Maryland

(Manuscript received 19 December 2005, in final form 8 May 2006)

ABSTRACT

The fidelity of the interannual variability of precipitation over Nordeste is examined using the suite of the NCEP Climate Forecast System (CFS) seasonal hindcasts. These are coupled ocean–land–atmosphere multiseasonal integrations. It is shown that the Nordeste rainfall variability in the season of February–April has relatively low skill in the CFS seasonal hindcasts. Although Nordeste is a comparatively small region in the northeast of Brazil, the analysis indicates that the model has a large-scale error in the tropical Atlantic Ocean. The CFS exhibits a widespread El Niño–Southern Oscillation (ENSO) forcing over the tropical Atlantic Ocean. As a consequence of this remote ENSO forcing, the CFS builds an erroneous meridional SST gradient in the tropical Atlantic that is known from observations to be a critical forcing for the rainfall variability over Nordeste.

1. Introduction

Nordeste or Northeast Brazil (Fig. 1) has been noted by many authors to be a region of high seasonal climate predictability (Misra 2006, 2004; Sun et al. 2005; Moura and Hastenrath 2004; Folland et al. 2001; Goddard et al. 2003; Oldenborgh et al. 2005). This primarily results from the strong influences of tropical Pacific and Atlantic Ocean variability (Nobre and Shukla 1996; Hastenrath and Greischar 1993). Numerical model prediction studies that heretofore have been conducted over Nordeste have either been performed in a psuedoforecast mode [where observed SST is prescribed to the atmospheric general circulation model (AGCM)] or in tier-2-type predictions where the AGCM is forced with forecast SST derived from an independent source. This study examines the prediction skill of precipitation during the rainy season of Nordeste in a coupled ocean–land–atmosphere forecast system.

Observational studies (Moura and Shukla 1981; Hastenrath and Heller 1977) have shown that tropical sea surface temperature anomaly (SSTA) over the Atlantic and the eastern Pacific Ocean modulates the Nordeste seasonal rainfall variability. More recently, with innovative modeling experiments, Giannini et al. (2001), Saravanan and Chang (2000), and Misra (2006) have attempted to separate the contributions of the variability in the Atlantic and Pacific Oceans to Nordeste rainfall variability. These studies clearly point out that the tropical Atlantic SST variability is critical in modulating the Nordeste rainfall variability. However, it should be noted that there is other evidence from observations (Nobre and Shukla 1996; Curtis and Hastenrath 1995; Enfield and Mayer 1997) and modeling studies (Saravanan and Chang 2000) to suggest that the Atlantic SST variability is strongly influenced by El Niño–Southern Oscillation (ENSO) in addition to its intrinsic variability (Chang et al. 2003; Giannini et al. 2001). Futhermore, this relationship between ENSO in the eastern equatorial Pacific Ocean and the northern tropical Atlantic Ocean (NTAO) SSTA has a lag of about one season (Enfield and Mayer 1997).

Observations and modeling studies suggest that it is the meridional gradient of SSTA in the tropical Atlantic Ocean that modulates the Nordeste rainfall variability (Moura and Shukla 1981; Nobre and Shukla 1996;

Corresponding author address: Dr. Vasubandhu Misra, Center for Ocean–Land–Atmosphere Studies, Institute of Global Environment and Society, Inc., 4041 Powder Mill Road, Suite 302, Calverton, MD 20705.
E-mail: misra@cola.iges.org

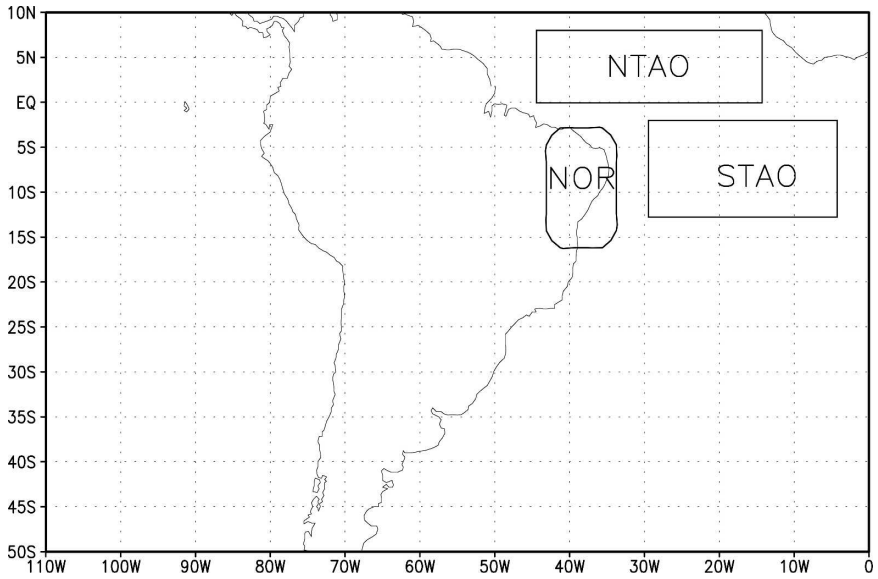

FIG. 1. The outline of the Nordeste area (NOR) in northeast Brazil is shown. The outline of areas denoting NTAO and STAO is also shown. NTAO and STAO areas are used to calculate the meridional gradient of SST in the tropical Atlantic Ocean.

Giannini et al. 2004; Misra 2006, among others). Although opposite-sign SSTAs often appear north and south of the equator in the Atlantic Ocean, giving them the appearance of a dipole, there is evidence to suggest that these anomalies may appear independently (Enfield and Mayer 1997; Mehta 1998; Dommenget and Latif 2000, 2002). The NTAO anomaly has been described as a manifestation of remote ENSO forcing (Czaja et al. 2002; Chiang et al. 2002; Huang et al. 2002), chaotic atmospheric variability, such as the North Atlantic Oscillation (Wallace et al. 1990; Czaja and Frankignoul 2002), and local air–sea thermodynamic feedback (Chang et al. 2003; Huang et al. 2004), while Hu and Huang (2005) provided a dynamical air–sea feedback mechanism to explain the appearance of SSTA in the southeastern Atlantic Ocean.

Giannini et al. (2004) and Misra (2006) used uncoupled AGCM experiments to show that the predictability of Nordeste rainfall is reduced when the meridional gradient of SSTA in the tropical Atlantic develops contrary to the ENSO forcing. That is, when the SSTA in the NTAO region is large and not significantly correlated with eastern Pacific Ocean SSTA, then the certainty of Nordeste rainfall variability is less obvious. This adds additional complexity to the predictability of Nordeste rainfall variability. In fact, Misra (2006) showed instances of poor seasonal predictability of rainfall over Nordeste even when the ENSO variability in the eastern Pacific is significantly large. More recently, Oldenborgh et al. (2005) showed that the European Centre for Medium-Range Weather Forecasts coupled seasonal forecast system had relatively higher skill in predicting Nordeste rainfall variability and outperformed an ENSO-based statistical model.

The purpose of this study is to analyze a huge set of seasonal hindcasts from the Coupled Forecast System (CFS) of the National Centers for Environmental Prediction (NCEP) that was recently developed and released to the community (Saha et al. 2006). CFS represents a growing perception in the community that coupled ocean–land–atmosphere models (which can, in principle, more faithfully represent the relevant coupled processes) should be developed and encouraged for the prediction of seasonal climate (see online at http://copes.ipsl.jussieu.fr/Organization/Activities/TFSeasonalPred.html). A reflection of this tenet is found in the motivation for the Development of a Multimodel Ensemble System for Seasonal to Interannual Climate Prediction project initiated in Europe (DEMETER; Palmer et al. 2004). This project demonstrated that coupled models have comparable or higher skill than the forced AGCM experiments in the first season (Gueremy et al. 2005; Graham et al. 2005; Oldenborgh et al. 2005), thus supporting the point that coupled ocean–land–atmosphere models have the capability to capture unrealized seasonal predictability that may arise from interactions among the climate components. Therefore, verifying and examining the Nordeste seasonal rainfall—a coupled ocean–atmosphere phenomenon—in the CFS is most appropriate.

The domain of Nordeste outlined in Fig. 1 is identical to that in Misra (2006). The season to be examined is February–April (FMA). Although the domain outlined for Nordeste extends into both the northern and the southern regions, which have been shown to have distinct variability and annual cycles (Moura and Shukla 1981), neither the Climate Prediction Center Merged Analysis Precipitation (CMAP; Xie and Arkin 1996) nor the CFS model at T62 spectral truncation are able to capture this feature. Furthermore, Misra (2006) showed that for this domain of Nordeste, the annual cycle of precipitation peaks in FMA. In addition, although the focus of the paper is on the Nordeste rainfall variability, the analysis points to a model bias at much larger scales.

In the following section, we will briefly outline the CFS followed by a concise description of the suite of hindcast experiments. The results are discussed in section 3 and the summary and concluding remarks are made in section 4.

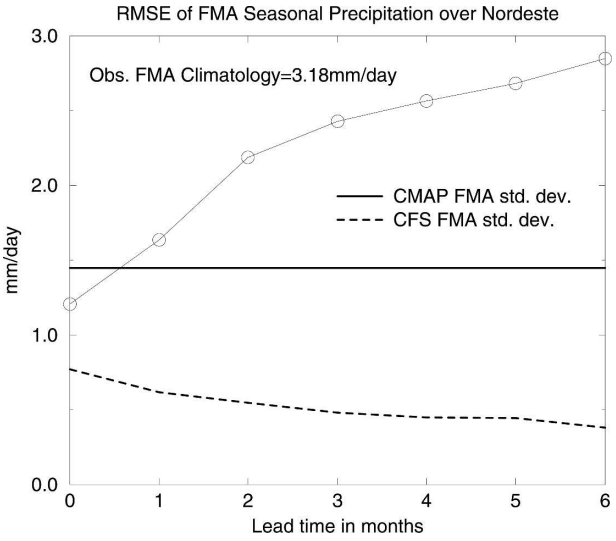

FIG. 2. The RMSE of the FMA seasonal mean rainfall over Nordeste. The observations are from CMAP (Xie and Arkin 1996). The interannual std devs from CMAP and CFS for FMA seasonal mean rainfall are also shown.

2. Description of the model and seasonal hindcasts

The CFS model, described in detail in Wang et al. (2005) and Saha et al. (2006), is summarized here. It is a 64-level, terrain-following (σ) vertical coordinate with T62 horizontal resolution (equivalent to an approximately 200-km grid) model. The AGCM of this coupled model is modified from the version adopted in the NCEP–National Center for Atmospheric Research (NCAR) reanalysis (Kalnay et al. 1996) with updates to the shortwave, boundary layer, cumulus convection, and gravity wave drag and with the inclusion of a new prognostic variable in the cloud water–ice scheme (Wang et al. 2005). The oceanic component of the CFS is the Geophysical Fluid Dynamics Laboratory (GFDL) Modular Ocean Model version 3 (MOM3; Pacanowski and Griffies 1998). It covers the global ocean from 74°S to 64°N. The zonal resolution is 1°. The meridional resolution is ⅓° between 10°S and 10°N, gradually increasing through the Tropics and getting fixed at 1° poleward of 30°S and 30°N. There are 40 layers in the vertical with 27 layers in the upper 400 m. The coupling between the atmospheric and the oceanic components is done once a day without any flux adjustment.

Saha et al. (2006) have given a detailed description of the suite of seasonal hindcasts from CFS produced by NCEP. There are 15 ensemble members for each seasonal hindcast integration (covering the period 1981–2003) starting from every month of the year through the following 9 months. It should be mentioned that in this study, model runs identified by their start month (lead month 1) include ocean initial state of the 11th and 21st of the lead month 0 and 1st of the lead month 1.

3. Results

In discussing the results of this study, we shall be using extensively the CMAP dataset (Xie and Arkin 1996) and the NCEP–NCAR reanalysis (Kalnay et al. 1996), made available on a 2.5° × 2.5° latitude–longitude grid, to verify and compare the model simulations. We shall also be using the SST from the Extended Reynolds and Smith SST version 2 (ERSST-V2; Smith and Reynolds 2005). The verification is made over a time period from 1981 to 2003. Furthermore, we shall be depicting the results from the ensemble mean (averaged over the 15 ensemble members) of the model runs.

In Fig. 2, we show the root-mean-square error (RMSE) of FMA rainfall as a function of lead time. This figure clearly indicates that the mean precipitation errors in the CFS over Nordeste depend on lead time. This is despite the known, strong observed teleconnections of Nordeste precipitation with slowly varying SST. Misra (2004) showed that seasonal hindcast and long multiyear integrations of an AGCM forced with observed SST had comparable skill over Nordeste, thus reinforcing the notion that seasonal rainfall predictability in Nordeste is unlikely to be an initial value problem. However, in a coupled model where the SST is also a prognostic variable, such a conclusion is not obvious. Rather, it is not surprising to see that precipita-

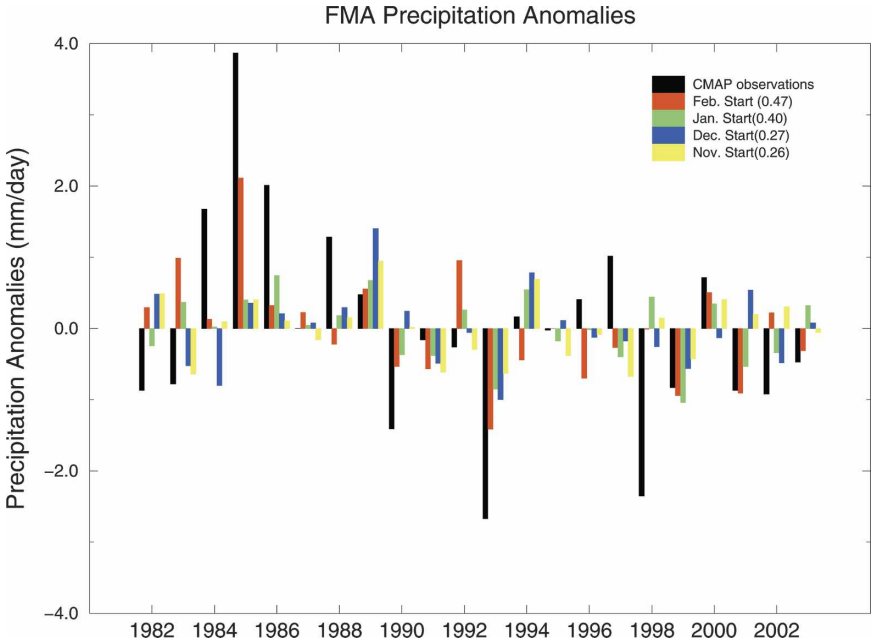

FIG. 3. FMA seasonal mean rainfall anomalies from observations (CMAP) and CFS hindcasts at 0- (February start), 1- (preceding January start), 2- (preceding December start), 3- (preceding November start), 4- (preceding October start), 5- (preceding September start), and 6- (preceding August start) month lead times. The anomaly correlations of the seasonal rainfall are indicated in the legend.

tion errors over Nordeste are a function of lead time. From zero lead time (February start) to a 6-month lead time (August start), the RMSE of the FMA seasonal mean rainfall grows from 1.3 to 2.8 mm day^{-1}, making it almost comparable to the observed seasonal mean climatology of 3.18 mm day^{-1} over the region. In Fig. 2, we also show the interannual standard deviations of FMA seasonal rainfall from CMAP and CFS as a function of lead time. It is clearly seen that the standard deviation of FMA seasonal rainfall is underestimated by the CFS and the variability reduces gradually as a function of lead time. In Fig. 3, we illustrate the mean FMA seasonal rainfall anomaly over Nordeste from observations and CFS from a lead time of 0–3. The anomaly correlations are relatively small compared to previous GCM studies forced with observed SST (Misra 2004, 2006; Folland et al. 2001). The main objective of this paper is to investigate the cause of this low skill in the CFS seasonal hindcasts.

The contemporaneous teleconnection of the Nordeste FMA seasonal rainfall with the tropical SST in the Pacific and Atlantic Ocean basins is shown in Figs. 4a,b from observations and from the corresponding seasonal hindcasts at 0- month lead time. A similar set of comparative figures (Figs. 4c,d) are shown with FMA seasonal Nordeste rainfall correlated against the preceding November–January (NDJ) SST. It should be mentioned that for generating Fig. 4d, we utilized the CFS seasonal hindcasts with a 3-month lead (November start). It is apparent from these figures that the teleconnections of Nordeste rainfall variability are erroneous in the CFS seasonal hindcasts. In the CFS (Fig. 4b), the variability in the south tropical Atlantic Ocean (STAO) clearly dictates a large proportion of the total predictable Nordeste rainfall variability contrary to observations both at zero and one season lag. On the other hand, the observations (Figs. 4a,c) indicate a subtle interplay of covariability between the eastern Pacific and the Atlantic SST gradient (set up between the NTAO and the STAO regions) that teleconnects to Nordeste rainfall variability. It should also be noted that Fig. 4a shows a significant correlation with the SST over the South Atlantic convergence zone region. However, there is insufficient observed data to verify this relationship further. At one seasonal lag (Fig. 4c), the observed correlations of the FMA seasonal rainfall over Nordeste with the SST of the preceding NDJ season are similar to the contemporaneous correlation pattern in Fig. 4a except that the correlations are relatively weaker. The appearance of this teleconnection pattern is consistent with the observational studies of Enfield and Mayer (1997) that indicate one season lag in the relationship between the NTAO SST and ENSO variability in the eastern Pacific Ocean. The CFS persists

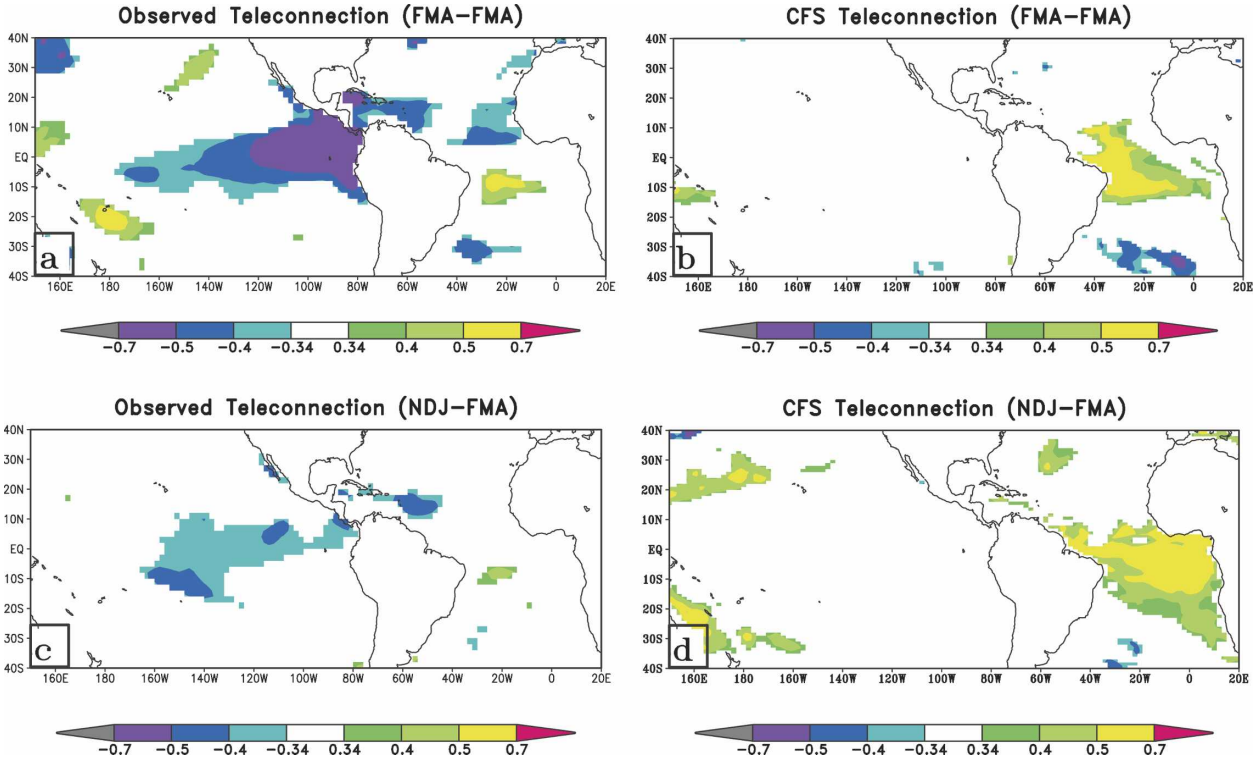

FIG. 4. The correlations of the Nordeste mean FMA seasonal precipitation anomaly from (a) observations (CMAP) with contemporaneous observed (ERSST-V2; Smith and Reynolds 2005) SST, (b) CFS with contemporaneous SST from February (0-month lead) start run, (c) observations with 1-season lead (NDJ) observed SST, and (d) CFS with 1-season lead (NDJ) SST from November (3-month lead) start run. Correlations at the 90% confidence limit are shaded.

with the erroneous positive correlations over the STAO region with the absence of any significant negative correlation over the tropical Pacific Ocean.

Similarly, in Fig. 5, we show the contemporaneous correlation of Niño-3 SST with global SST from observations and the corresponding CFS seasonal hindcasts (at zero lead time) for the FMA season. In the observations (Fig. 5a), the relationship of the NTAO SST anomalies with ENSO variability is clearly seen. This supports the theory that NTAO SST anomalies are a manifestation of remote ENSO forcing. However, the absence of any contemporaneous (or even at one season lag; not shown) correlations over the STAO region indicates that the SST anomalies in this region are unlikely to be related to remote ENSO forcing. Yet, the CFS displays correlations that stretch into both hemispheres and are basinwide over the tropical Atlantic in contrast to observations. In other words, the ENSO effect over the tropical Atlantic Ocean is erroneous in the CFS. This consequently results in an erroneous development of the anomalous meridional gradient of SST in the tropical Atlantic Ocean. This is further illustrated in Fig. 6a (Fig. 6b) where we show the regression of the meridional gradient of the mean FMA (leading NDJ) SST against global precipitation from observations. The meridional gradient of tropical Atlantic SST is calculated as the difference between the area-averaged SST over the northern and the southern tropical Atlantic regions (NTAO and STAO regions) outlined in Fig. 1. This figure shows an inverse relationship (significant at 90% according to a t test) that evolves from central Nordeste with the meridional gradient of SST leading by one season (Fig. 6a) to northern Nordeste (Fig. 6b) with the contemporaneous SST over the tropical Atlantic Ocean. A similar figure for the CFS (not shown) indicated an absence of any significant relationship of the tropical Atlantic SST gradient on the Nordeste FMA seasonal rainfall anomaly.

A related significant problem in the CFS is the erroneous symmetric response about the equator of the lower-tropospheric temperature to ENSO heating (Figs. 7a,b). In Figs. 7a,b, we have plotted the correlation of the Niño-3 seasonal mean (NDJ) anomaly of SST with the succeeding 850-hPa-temperature seasonal mean anomaly (FMA) from the NCEP–NCAR reanalysis and the CFS seasonal hindcasts starting in November, respectively. The correlation patterns are symmetric and comparable in the two figures over the

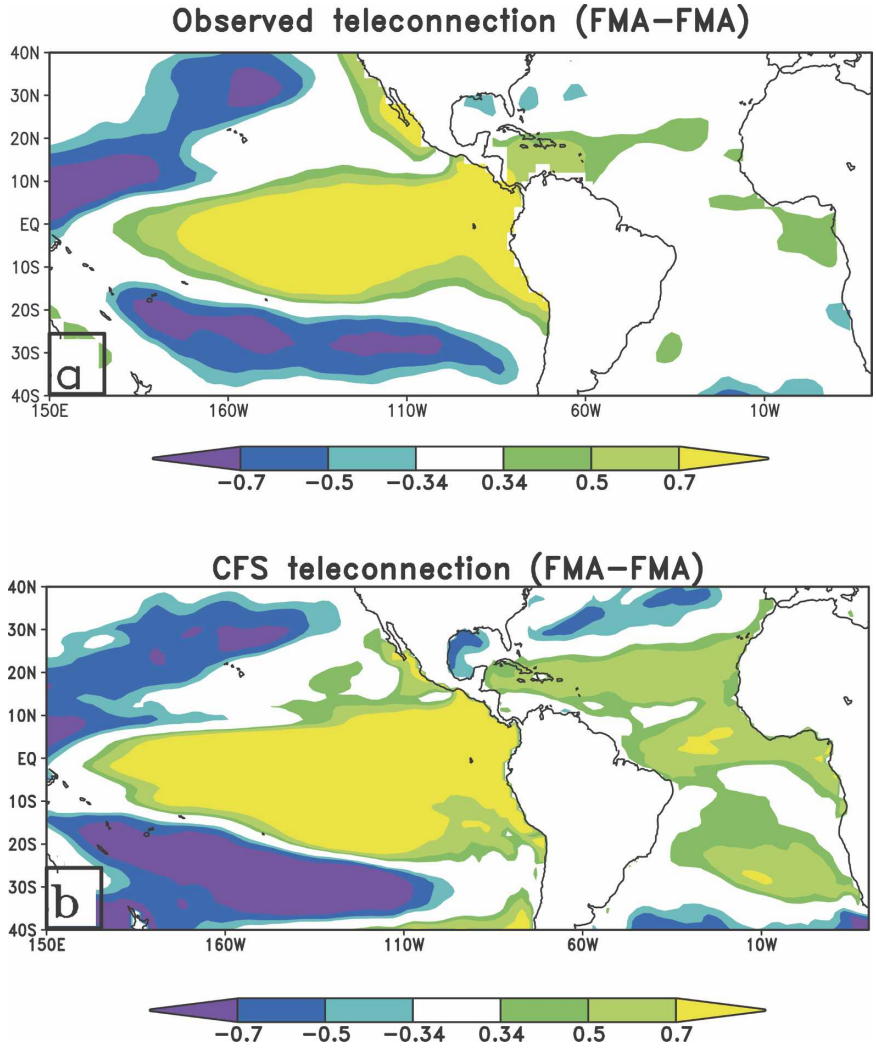

FIG. 5. The correlations of the Niño-3 mean FMA SST with contemporaneous observed SST from (a) observations (ERSST-V2) and (b) CFS from February (0-month lead) start runs. Correlations at the 10% significance level according to *t* tests are shown.

tropical Pacific. However, over the tropical Atlantic Ocean, the NCEP–NCAR reanalysis exhibits an asymmetric pattern with stronger correlations over the Caribbean Sea that is farther northwestward. In the CFS, the correlations are nearly symmetric about the equator over the Atlantic Ocean. This has implications on the simulated SST anomalies in the CFS following the Brown and Bretherton (1997) argument. They showed that externally forced tropospheric temperature (TT) anomalies in convective regions affect the boundary layer equivalent potential temperature since it is locked to a virtual temperature profile in a quasi-equilibrium state. In a related study, Chiang and Sobel (2002) showed from their idealized experiments that the tropospheric temperature anomalies propagate to the surface only in regions of convection, which could either be deep or shallow. Since the free atmosphere in the tropical latitudes cannot maintain horizontal pressure gradients, the TT anomalies are uniform in response to ENSO SST anomalies in the equatorial Pacific (Yulaeva and Wallace 1994). As a result, the equivalent potential temperature in the boundary layer is forced to change in the convective regions of the global Tropics that include the southern tropical Atlantic region as a response to the remote ENSO forcing. Huang and Hu (2005), in analyzing the systematic errors over the tropical Atlantic Ocean in the CFS, indicated an excessive warming of the SST under the southern branch of the ITCZ that arises from an excessive downwelling shortwave flux as a result of the model's inability to produce adequate low-level cloud cover in the region. As a consequence of the Brown and Bretherton (1997)

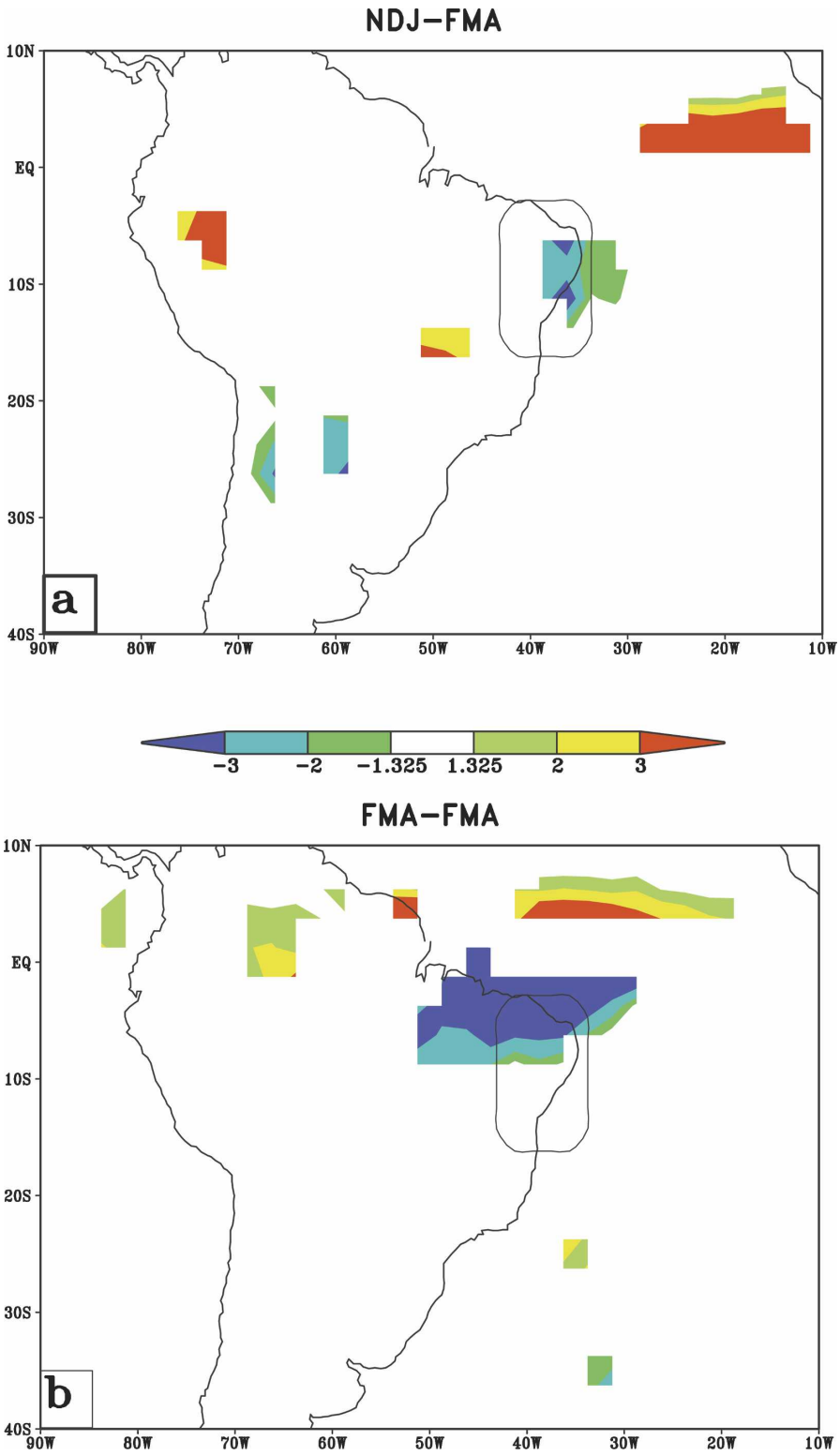

FIG. 6. The observed regression of the (a) leading NDJ and (b) FMA seasonal mean meridional gradient of SST in the tropical Atlantic with the FMA seasonal global precipitation (CMAP). The units are in mm day^{-1}. The domain of Nordeste is also outlined. The meridional gradient of SST is calculated as the difference in the area-averaged SST over the NTAO and STAO regions outlined in Fig. 1.

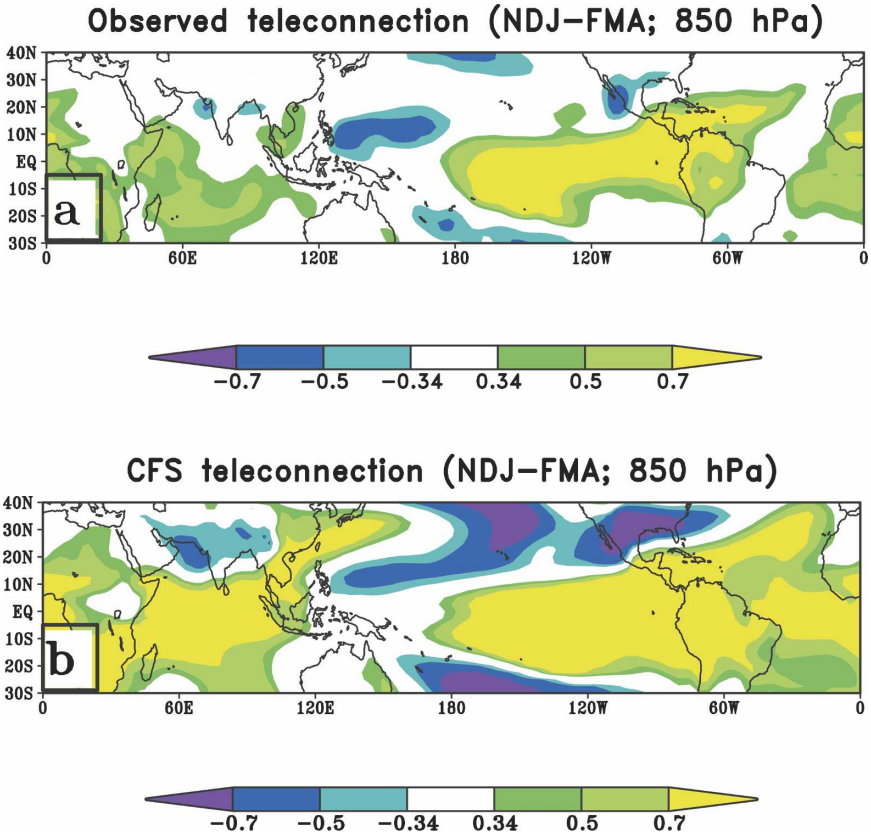

FIG. 7. The correlation of leading mean NDJ Niño-3 SST from (a) observations with mean temperature at 850 hPa from the NCEP–NCAR reanalysis and (b) CFS seasonal hindcasts with the mean seasonal (FMA) temperature at 850 hPa from the November (3-month lead) start runs. Correlations at the 10% significance level are indicated.

mechanism and the warm SST bias over the STAO region in the CFS, the convection is overtly active over the southern branch of the ITCZ, resulting in erroneous symmetric TT anomalies. It should, however, be mentioned that the correlations of the Niño-3 SST with the temperature anomalies above 300 hPa are symmetric about the equator in the Atlantic both in the NCEP–NCAR reanalysis and in the CFS (not shown).

4. Conclusions

The National Centers for Environmental Prediction (NCEP) Climate Forecast System (CFS) has been evaluated for its fidelity of Nordeste seasonal rainfall variability in the February–April season. The suite of seasonal hindcasts comprising 15 ensemble members for coupled integrations starting from each month of the year exhibit relatively low skill over Nordeste, despite the relatively high predictability of that region's rainy season.

The CFS is a huge improvement in ENSO simulation and prediction (Wang et al. 2005; Saha et al. 2006) over other dynamical systems, and its hindcast skill over the Niño-3 region is comparable to the best statistical models. Yet, its ENSO teleconnection pattern over the tropical Atlantic Ocean is at variance with observations. In this study we find that in the CFS, the Niño-3 SST teleconnection with the tropical Atlantic SST in the February–April season is widespread, extending into both hemispheres and being basinwide. As a result, the anomalous meridional gradient of SST in the tropical Atlantic in the CFS is erroneous. Consequently, the skill of the Nordeste seasonal rainfall variability in the CFS seasonal hindcasts is poor, as it is critically dependent on this anomalous meridional gradient of SST in the tropical Atlantic.

It is also shown in this study that the seasonal tropospheric temperature anomalies in the lower troposphere (850 hPa) are symmetric about the equator in the Atlantic Ocean, contrary to that exhibited by the NCEP–NCAR reanalysis. This is further accentuated by the split ITCZ phenomenon in the CFS that is indi-

cated in the study of Huang and Hu (2005). Similar problems over the tropical Atlantic Ocean have been identified in other coupled models (Huang et al. 2004; Davey et al. 2002). The interannual variability in the Atlantic Ocean is a fine balance between the intrinsic and the forced variability (Chang et al. 2003; Huang et al. 2004). Obviously, when models show strong ENSO variability such as in the CFS, the relative roles of the forced and intrinsic variations change, giving rise to unverifiable variability. In this study we show that through the tropospheric temperature mechanism of Brown and Bretherton (1997), a widespread ENSO response can further exacerbate the remote ocean response that is already influenced by the prevalent systematic errors.

Nordeste in northeast Brazil is a region of relatively high seasonal climate predictability in forced AGCM simulations or in two-tier forecast systems. This study reveals that despite the strong observed teleconnections of the slowly varying SST on the Nordeste climate variability, the systematic errors and erroneous coupled feedback mechanisms offer a stiff challenge for making coupled models an invaluable tool for climate prediction.

Acknowledgments. The authors are greatly indebted to an anonymous reviewer who pointed to a glaring mistake in an earlier draft of this manuscript, which led to overall improvement. The authors thank Dr. Bohua Huang for useful discussions during the course of this work. The authors also thank Jim Kinter for his review comments on this work. The authors also thank NCEP for making the CFS hindcast data available and Jennifer Adams for assisting with the processing and analysis of the data. This study was supported by NSF Grant ATM9814295, NASA Grant NAG5-11656, and NOAA Grant NA16GP2248.

REFERENCES

Brown, R. G., and C. S. Bretherton, 1997: A test of the strict quasi-equilibrium theory on long time and space scales. *J. Atmos. Sci.,* **54,** 624–638.

Chang, P., R. Saravanan, and L. Ji, 2003: Tropical Atlantic seasonal predictability: The roles of El Niño remote influence and thermodynamic air–sea feedback. *Geophys. Res. Lett.,* **30,** 1501, doi:10.1029/2002GL016119.

Chiang, J. C. H., and A. Sobel, 2002: Tropical tropospheric temperature variations caused by ENSO and their influence on the remote tropical climate. *J. Climate,* **15,** 2616–2631.

——, Y. Kushnir, and A. Giannini, 2002: Deconstructing Atlantic Intertropical Convergence Zone variability: Influence of the local cross-equatorial sea surface temperature gradient and remote forcing from the eastern equatorial Pacific. *J. Geophys. Res.,* **107,** 4004, doi:10.1029/2000JD000307.

Curtis, S., and S. Hastenrath, 1995: Forcing of anomalous sea surface temperature evolution in the tropical Atlantic during Pacific warm events. *J. Geophys. Res.,* **100,** 15 835–15 847.

Czaja, A., and C. Frankignoul, 2002: Observed impact of Atlantic SST anomalies on the North Atlantic Oscillation. *J. Climate,* **15,** 606–623.

——, P. van der Vaart, and J. Marshall, 2002: A diagnostic study of the role of remote forcing in tropical Atlantic variability. *J. Climate,* **15,** 3280–3290.

Davey, M., and Coauthors, 2002: STOIC: A study of coupled model climatology and variability in tropical ocean regions. *Climate Dyn.,* **18,** 403–420.

Dommenget, D., and M. Latif, 2000: Interannual to interdecadal variability in the tropical Atlantic. *J. Climate,* **13,** 777–792.

——, and ——, 2002: A cautionary note on the interpretation of EOFs. *J. Climate,* **15,** 216–225.

Enfield, D. B., and D. A. Mayer, 1997: Tropical Atlantic sea surface temperature variability and its relation to El Niño–Southern Oscillation. *J. Geophys. Res.,* **102,** 929–945.

Folland, C. K., A. W. Colman, D. P. Rowell, and M. K. Davey, 2001: Predictability of northeast Brazil rainfall and real-time forecast skill, 1987–98. *J. Climate,* **14,** 1937–1958.

Goddard, L., A. G. Barnston, and S. J. Mason, 2003: Evaluation of the IRI's "net assessment" seasonal climate forecasts: 1997–2001. *Bull. Amer. Meteor. Soc.,* **84,** 1761–1781.

Giannini, A., J. C. H. Chang, M. A. Cane, Y. Kushnir, and R. Seager, 2001: The ENSO teleconnection of the tropical Atlantic Ocean: Contributions of the remote and local SSTs to rainfall variability in the tropical Americas. *J. Climate,* **14,** 4530–4544.

——, R. Saravanan, and P. Chang, 2004: The preconditioning role of tropical Atlantic variability in the development of the ENSO teleconnection: Implications for the prediction of Nordeste rainfall. *Climate Dyn.,* **22,** doi:10.1007/s00382-004-0420-2.

Graham, R. J., M. Gordon, P. J. Mclean, S. Ineson, M. R. Huddleston, M. K. Davey, A. Brookshaw, and R. T. H. Barnes, 2005: A performance comparison of coupled and uncoupled versions of the Met Office seasonal prediction general circulation model. *Tellus,* **57A,** 320–339.

Gueremy, J.-F., M. Deque, A. Braun, and J.-P. Piedelievre, 2005: Actual and potential skill of seasonal predictions using the CNRM contribution to DEMETER: Coupled versus uncoupled model. *Tellus,* **57A,** 308–319.

Hastenrath, S., and L. Heller, 1977: Dynamics of climate hazards in northeast Brazil. *Quart. J. Roy. Meteor. Soc.,* **103,** 77–92.

——, and L. Greischar, 1993: Further work on the prediction of northeast Brazil rainfall anomalies. *J. Climate,* **6,** 743–758.

Hu, Z.-Z., and B. Huang, 2005: Physical processes associated with the tropical Atlantic SST gradient. Part I: The thermodynamical mode in boreal spring. COLA Tech. Rep. 189, 39 pp. [Available online at ftp://grads.iges.org/pub/ctr/ctr_189.pdf.]

Huang, B., and Z.-Z. Hu, 2005: Evolution of model systematic errors in the tropical Atlantic basin from the NCEP coupled hindcasts. COLA Tech. Rep. 198, 45 pp. [Available online at ftp://grads.iges.org/pub/ctr/ctr_198.pdf.]

——, P. S. Schopf, and Z. Pan, 2002: The ENSO effect on the tropical variability. A regionally coupled model study. *Geophys. Res. Lett.,* **29,** 2039, doi:10.1029/2002GL014872.

——, ——, and J. Shukla, 2004: Intrinsic ocean–atmosphere variability in the tropical Atlantic Ocean. *J. Climate,* **17,** 2058–2077.

Kalnay, E., and Coauthors, 1996: The NCEP/NCAR 40-Year Reanalysis Project. *Bull. Amer. Meteor. Soc.,* **77,** 437–471.

Mehta, V. M., 1998: Variability of the tropical ocean surface temperatures at decadal–multidecadal time scales. Part I: The Atlantic Ocean. *J. Climate,* **11,** 2351–2375.

Misra, V., 2004: An evaluation of the predictability of austral summer season precipitation over South America. *J. Climate,* **17,** 1161–1175.

——, 2006: Understanding the predictability of seasonal precipitation over northeast Brazil. *Tellus,* **58A,** 307–319.

Moura, A. D., and J. Shukla, 1981: On the dynamics of droughts in northeast Brazil: Observations, theory, and numerical experiments with a general circulation model. *J. Atmos. Sci.,* **38,** 2653–2675.

——, and S. Hastenrath, 2004: Climate prediction for Brazil's Nordeste: Performance of empirical and numerical modeling methods. *J. Climate,* **17,** 2667–2672.

Nobre, C., and J. Shukla, 1996: Variations of sea surface temperature, wind stress, and rainfall over the tropical Atlantic and South America. *J. Climate,* **9,** 2464–2479.

Pacanowski, R. C., and S. M. Griffies, 1998: MOM3.0 manual. NOAA/Geophysical Fluid Dynamics Laboratory, Princeton, NJ, 561 pp.

Palmer, T. N., and Coauthors, 2004: Development of a European Multimodel Ensemble System for Seasonal-to-Interannual Prediction (DEMETER). *Bull. Amer. Meteor. Soc.,* **85,** 853–872.

Saha, S., and Coauthors, 2006: The NCEP climate forecast system. *J. Climate,* **19,** 3483–3517.

Saravanan, R., and P. Chang, 2000: Interaction between tropical Atlantic variability and El Niño–Southern Oscillation. *J. Climate,* **13,** 2177–2194.

Smith, T. M., and R. W. Reynolds, 2005: A global merged land–air–sea surface temperature reconstruction based on historical observations (1880–1997). *J. Climate,* **18,** 2021–2036.

Sun, L., D. F. Moncunill, H. Li, A. D. Moura, and F. A. S. Filho, 2005: Climate downscaling over Nordeste, Brazil, using the NCEP RSM97. *J. Climate,* **18,** 551–567.

van Oldenborgh, G. J., M. A. Balmaseda, L. Ferranti, T. N. Stockdale, and D. L. T. Anderson, 2005: Evaluation of atmospheric fields from the ECMWF seasonal forecasts over a 15-year period. *J. Climate,* **18,** 3250–3269.

Wallace, J. M., C. Smith, and Q. Jiang, 1990: Spatial patterns of atmosphere-ocean interaction in the Northern Hemisphere. *J. Climate,* **3,** 990–998.

Wang, W., S. Saha, H.-L. Pan, S. Nadiga, and G. White, 2005: Simulation of ENSO in the new NCEP Coupled Forecast System Model (CFS03). *Mon. Wea. Rev.,* **133,** 1574–1593.

Xie, P., and P. Arkin, 1996: Analysis of global monthly precipitation using guage observations, satellite estimates, and numerical model predictions. *J. Climate,* **9,** 840–858.

Yulaeva, E., and M. Wallace, 1994: The signature of ENSO in global temperature and precipitation fields derived from the microwave sounding unit. *J. Climate,* **7,** 1719–1736.